1534
doi:10.1017/S1431927618008152
Microsc. Microanal. 24 (Suppl 1), 2018

Atomic-Level Characterization of Thermoelectric $La_{1/3}NbO_3$

Demie Kepaptsoglou[1], Jakub D. Baran[2], Feridoon Azough[3], Marco Molinari[2,3], Stephen C. Parker[2], Robert Freer and Quentin M. Ramasse[1]

[1.] SuperSTEM Laboratory, SciTech Daresbury Campus, Daresbury WA4 4AD, U.K.
[2.] Department of Chemistry, University of Bath, Claverton Down, Bath BA2 7AY, U.K.
[3.] School of Materials, University of Manchester, Manchester, M13 9PL, U.K.
[4.]Department of Chemistry, University of Huddersfield, Huddersfield HD1 3DH, U.K.

There are limited numbers of ceramic compositions suitable for high-temperature thermoelectric (TE) applications. [1] The most promising candidates include $SrTiO_3$ based perovskites, due to their high Seebeck coefficient and a simple perovskite structure, which easily lends itself to doping and thus to tailoring of its electron- and thermal-transport properties.[2] However, one their main the drawbacks of is their high thermal conductivity which has a strong temperature dependence. In the search for new oxides with low thermal conductivities, which could be used on their own as new materials or in conjunction with STO as binary systems, we have identified A-site deficient perovskites as systems with great potential in TE applications and in particular the $La_{1/3}NbO_3$ ceramic his presents the highest vacancy content among the A-site-deficient perovskite family (whereby 2/3 of the A sites are vacant), a feature which may promote glasslike low thermal conductivity [3].

Here, we use aberration-corrected scanning transmission electron microscopy (STEM) and electron energy loss spectroscopy (EELS) to validate at the atomic scale structure of LNO and determine precisely the cation distribution in the structure, which has an important impact on the macroscopic properties of the ceramic. Crystallographic data from X-ray and electron diffraction confirmed that the room temperature structure is orthorhombic with *Cmmm* as a space group. Atomically resolved imaging and analysis showed that there are two distinct A sites: one (A_1) is occupied with La and vacancies, and the second site (A_2) is fully unoccupied (Figure 1 &2). Further imaging and EELS analysis reveals that the A1-site vacancies are not uniformly distributed across the A1 site but pair in lines appear to be lying in lines parallel to the $[1\bar{1}1]$ and $[11\bar{1}]$ directions.

First-principles electronic structure calculations are used to link the temperature dependence of the Seebeck coefficient measured experimentally to the evolution of the density of states with temperature and indicate possible avenues for further optimization through electron doping and control of the A-site occupancies. The calculations informed by structural characterization eveal that the $La_{1/3}NbO_3$ ceramic possesses a desirable band structure for n-type TE materials. Moreover, lattice thermal conductivity calculations give insights into the asymmetric dependence of the thermal conductivity on specific crystallographic directions of the material, which could be exploited via nanostructuring to create high-efficiency compound thermoelectrics.

References:
[1] K. Koumoto, K. Y Wang, R. Zhang, et al Annu. Rev. Mater. Res. **40** (2010) p.363
[2] D. Srivastava, C. Norman, F. Azough, et al Phys. Chem. Chem. Phys. 18 (2016), 26475
[3] D. Kepaptsoglou, J. Baran, F. Azough et al, Inorg. Chem. **57** (2018) p.45
[4] SuperSTEM is the U.K. National Facility of Advanced Electron Microscopy funded by EPSRC

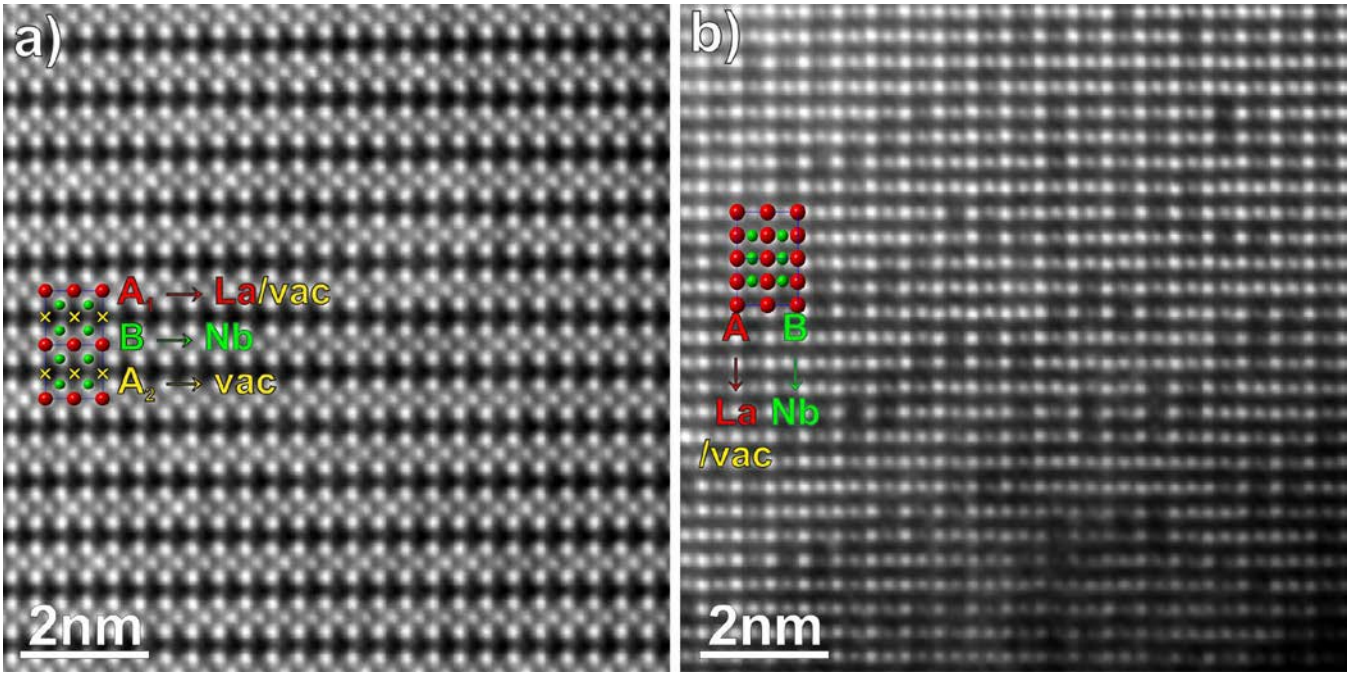

Figure 1. HAADF STEM images of the LNO ceramic acquired along the (a) [100] and (b) [101] zone axes. The corresponding ball-and-stick models of the LNO *Cmmm* structure are overlaid on the images for comparison (where yellow × symbols denote the vacant A_2 sites).

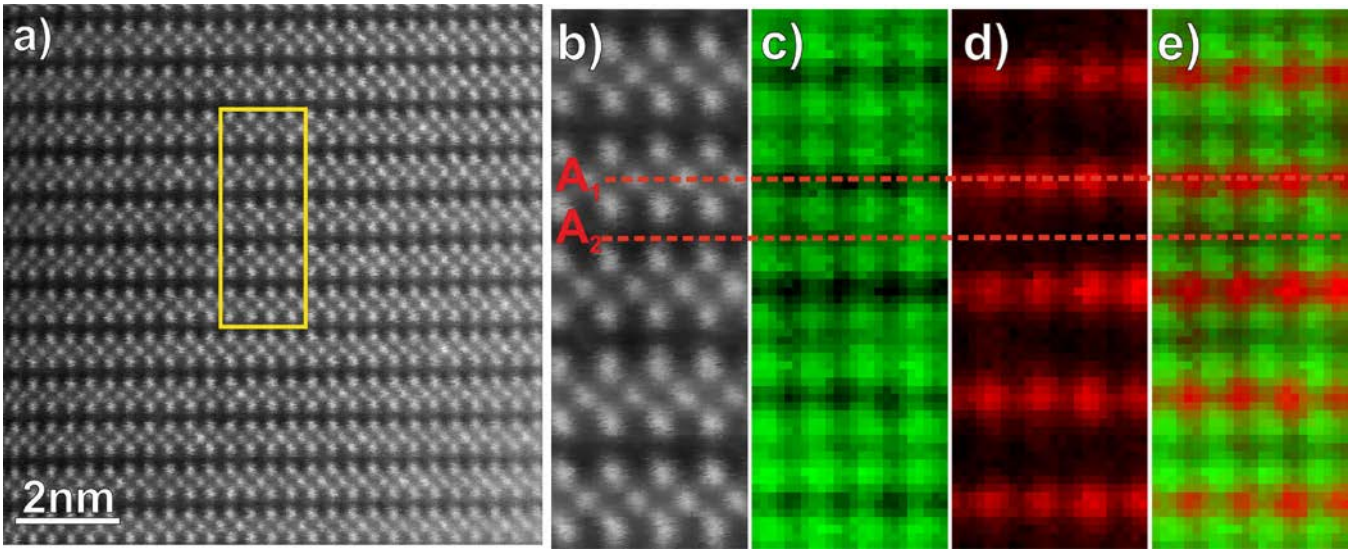

Figure 2. a) HAADF STEM survey image of $La_{1/3}NbO_3$ acquired along the [001] zone axis, showing the area used for analysis marked by a yellow rectangle; b) HAADF STEM signal intensity acquired simultaneously with the EELS signal; c,d) integrated EELS intensity map of the Nb $L_{2,3}$ and La $M_{4,5}$-edges, respectively and e) RGB overlay of (c) and (d).

https://doi.org/10.1017/S1431927618008152 Published online by Cambridge University Press